

A. Belousov · M. Belousova · B. Voight

Multiple edifice failures, debris avalanches and associated eruptions in the Holocene history of Shiveluch volcano, Kamchatka, Russia

Received: 28 June 1998 / Accepted: 28 March 1999

Abstract Investigation of well-exposed volcanoclastic deposits of Shiveluch volcano indicates that large-scale failures have occurred at least eight times in its history: approximately 10,000, 5700, 3700, 2600, 1600, 1000, 600 ¹⁴C BP and 1964 AD. The volcano was stable during the Late Pleistocene, when a large cone was formed (Old Shiveluch), and became unstable in the Holocene when repetitive collapses of a portion of the edifice (Young Shiveluch) generated debris avalanches. The transition in stability was connected with a change in composition of the erupting magma (increased SiO₂ from ca. 55–56% to 60–62%) that resulted in an abrupt increase of viscosity and the production of lava domes. Each failure was triggered by a disturbance of the volcanic edifice related to the ascent of a new batch of viscous magma. The failures occurred before magma intruded into the upper part of the edifice, suggesting that the trigger mechanism was indirectly associated with magma and involved shaking by a moderate to large volcanic earthquake and/or enhancement of edifice pore pressure due to pressurised juvenile gas. The failures typically included: (a) a retrogressive landslide involving backward rotation of slide blocks; (b) fragmentation of the leading blocks and their transformation into a debris avalanche, while the trailing slide blocks decelerate and soon come to rest; and (c) long-distance runout of the avalanche as a transient wave of debris with yield strength that glides on a thin weak

layer of mixed facies developed at the avalanche base. All the failures of Young Shiveluch were immediately followed by explosive eruptions that developed along a similar pattern. The slope failure was the first event, followed by a plinian eruption accompanied by partial fountain collapse and the emplacement of pumice flows. In several cases the slope failure depressurised the hydrothermal system to cause phreatic explosions that preceded the magmatic eruption. The collapse-induced plinian eruptions were moderate-sized and ordinary events in the history of the volcano. No evidence for directed blasts was found associated with any of the slope failures.

Key words Failure of volcanic edifice · Debris avalanche · Lava dome · Plinian eruption · Shiveluch volcano · Kamchatka

Introduction

The 1980 eruption of Mount St. Helens clearly demonstrated that a volcanic edifice can be destroyed in a large-scale slope failure, resulting in a destructive, fast-moving debris avalanche that travels a long distance (Voight et al. 1981; Glicken 1986, 1998). The Mount St. Helens avalanche deposit displays a hummocky landscape and distinctive features that enabled old debris-avalanche deposits to be recognised in volcanic regions worldwide (Ui 1983; Siebert 1984). Thus, it was discovered that large-scale slope failures were common events in the history of many volcanoes, and that some volcanoes experience multiple failures (Inokuchi 1988; Beget and Kienle 1992; Komorowski et al. 1993; Siebert et al. 1995; Belousov and Belousova 1996; Belousova 1994, 1996).

Most of the newly discovered old debris-avalanche deposits had been earlier misinterpreted, usually as moraines or lahar deposits. In the Kurile-Kamchatka region of Russia, some debris-avalanche deposits, including several at Shiveluch volcano, had been de-

Editorial responsibility: D. A. Swanson

Alexander Belousov (✉) · Marina Belousova
Institute of Volcanic Geology and Geochemistry,
Petropavlovsk-Kamchatsky, 683006, Russia
e-mail: A.Belousov@g23.relcom.ru
Fax: +095-7193776

Barry Voight
Department of Geosciences, Pennsylvania State University,
University Park, PA 16802, USA

Present address: Alexander Belousov, Vavilova str, 31/1–28,
Moscow, 117312, Russia

scribed as “directed blast agglomerates” (Gorshkov and Dubik 1970). This description emerged from early work on the deposits of the powerful explosive eruption of Bezymianny volcano in 1956, where crushed and transported rocks of the old edifice were interpreted as material ejected by the explosion (Gorshkov 1959). However, restudy of the Bezymianny deposit (Belousov and Bogoyavlenskaya 1988; Belousov and Belousova 1998) has shown that the so-called directed blast agglomerate is actually the deposit of a slope failure that immediately preceded the catastrophic directed blast, as at Mount St. Helens. The evidence that similar deposits at Shiveluch volcano also had a landslide origin was given for the first time in publications of the Belousova (1994, 1996). In this paper we provide further evidence to support this conclusion.

Slope failures at Shiveluch have occurred frequently and have regularly been associated with explosive volcanism. Because of the large number of avalanche deposits and related eruptive products found at Shiveluch, and the excellent exposures, study of these deposits might shed light on the connections between slope failures and associated volcanism. Removal of a large portion of the volcanic edifice as a result of slope failure can destabilise underlying magmatic or hydrothermal systems, in some cases causing catastrophic magmatic directed blasts (Hoblitt et al. 1981; Moore and Sisson 1981; Waitt 1981; Belousov 1996; Belousov and Belousova 1998), and in other cases plinian eruptions (Belousov 1995; Belousov and Belousova 1996), phreatic explosions (Sekiya and Kikuchi 1889) or no eruptions at all (Voight and Sousa 1994). The reasons for these different responses to large-scale slope failure are related to different conditions within a particular volcanic edifice prior to the failure (Voight et al. 1981, 1983; Siebert et al. 1987; Belousov 1995), but details of the process have not been clear. We hoped to gain an improved understanding of this question by study of the deposits at Shiveluch.

The aims of this paper are: (a) to document the stratigraphic relations and characterise the deposits of multiple slope failures and debris avalanches of Shiveluch volcano; (b) to evaluate the mechanisms of their origin, transportation and deposition; (c) to assess the trigger mechanisms for the slope failures; and (d) to determine the character of the associated eruptions in order to establish constraints that determined eruption type.

Morphology, edifice geology and modern activity

Shiveluch (in some literature, Sheveluch) is the northernmost active volcano of the Kamchatka peninsula, Russian Far East (Fig. 1). The volcano forms a large isolated edifice surrounded by lowlands of the northern part of the Central Kamchatka depression. The edifice has two main parts, referred to as Old Shiveluch and Young Shiveluch (Menyailov 1955; Melekestsev et al. 1991).

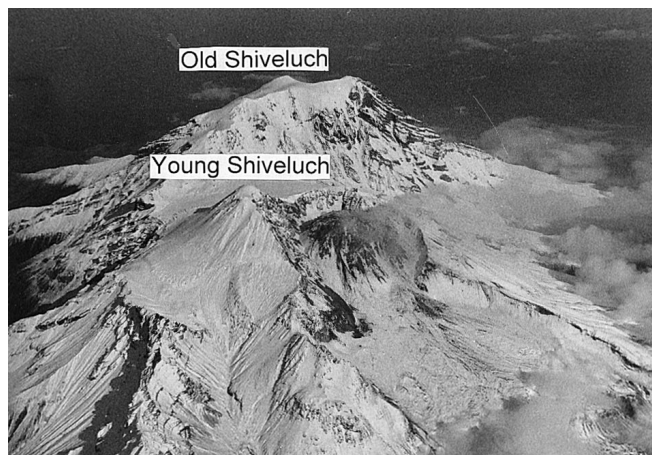


Fig. 1 Shiveluch volcano from the southwest, October 1994. Giant, 7-km-wide, horseshoe-shaped avalanche caldera of Old Shiveluch opens widely to the south. Edifice of Young Shiveluch, located inside the caldera, has its own horseshoe-shaped crater formed in 1964. Degassing 1980–1994 dome complex is nested in the crater. “Steps” – last portion of 1964 failure, stopped in the breach of the crater – are obscured by clouds in lower right corner. Note multiple long lava flows exposed in the wall of Old Shiveluch caldera, contrasting with pelean-type domes and short lava flows of Young Shiveluch

Old Shiveluch comprises the ruins of a giant stratovolcano of Pleistocene age, which was more than 4000 m high before its destruction. Its modern height is 3335 m (Fig. 2). The southern sector of the stratovolcano is truncated by a giant horseshoe-shaped caldera, more than 7 km wide, broadly open to the south.

A thick sequence of basaltic and andesitic pyroclastic layers is exposed in the base of the caldera wall. The eastern sector of caldera wall is 1500 m high, very steep and exposes more than ten andesitic lava flows, each up to 50–100 m thick and 3–5 km long. The flows were erupted from the summit region of Old Shiveluch volcano, in the location now occupied by the caldera. Possibly the uppermost lava flow was erupted at the very beginning of the Holocene after the end of the last glaciation, because parts of its surface were not eroded by glaciers and retain primary features. The northern sector of the caldera wall is almost completely buried by lava flows and talus of the Young Shiveluch edifice, but a small exposed part of the wall exhibits strongly altered rocks near the vent area of Old Shiveluch. The western wall of the caldera, approximately 500 m high, is composed of multiple thin (<20 m) and long (up to 15 km) lava flows of basaltic andesite. Probably most of these flows were fed by dikes of northeast orientation, which are now exposed in the caldera wall. A cluster of andesitic domes is situated on the western slope of Old Shiveluch volcano. These domes probably formed in the Holocene, because they have fresh uneroded forms and still display weak fumarolic activity.

Modern eruptions of the volcano originated only from Young Shiveluch, a ~2760-m-high Holocene cone nested inside the horseshoe-shaped caldera of Old

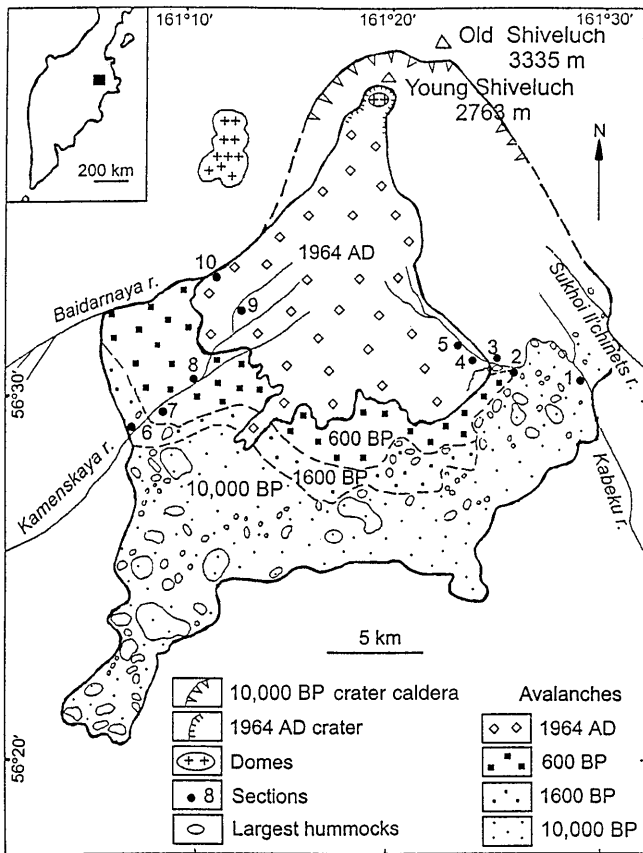


Fig. 2 Map of debris-avalanche deposits of Shiveluch volcano. Dashed lines delineate approximate margins of 1600- and 600-BP debris-avalanche deposits. Only locations of key sections are shown

Shiveluch (Figs. 1, 2). The cone consists mostly of plean domes and of short (<2 km), thick lava flows of andesitic composition. The lava flows and domes of Young Shiveluch are richer in silica (59.5–62.5%) than those of Old Shiveluch (54.5–56.5%), and other elements and mineralogical compositions are also notably different (Dril 1988).

When the volcanological observatory in nearby Kliuchi village was established in 1935, and monitoring began, Young Shiveluch contained a horseshoe-shaped crater approximately 1.5 km in width, open to the south. A plean-type lava dome occupied the crater. Historical reports suggest that this crater was formed or notably modified during the 1854 eruption, and the dome was formed in 1925–1930. In 1946–1949 a new lava dome (named Suelich) with a volume 0.9 km^3 was extruded in the crater (Menyailov 1955). It was adjacent to the old one, and together they filled the 1854 crater. In 1964 the Young Shiveluch dome complex collapsed, accompanied by a plinian eruption and the deposition of pumiceous pyroclastic flows (Belousov 1995). The newly formed horseshoe-shaped crater almost coincided with the crater of 1854, but a small scar of the old crater is still visible along the eastern rim of the

1964 crater. The 1964 explosive eruption was not immediately followed by formation of a lava dome, but later dome-forming eruptions in 1980–1981 and 1993–1994 resulted in a new plean lava dome complex with a volume of approximately 0.2 km^3 (Firstov et al. 1995; Dvigo 1995).

The breach of the Old Shiveluch caldera opens into a gentle, locally dissected, south-sloping plain (Fig. 2). For up to 15 km from the crater, most of the plain is mantled by unvegetated deposits of the 1964 eruption (debris avalanche and pumiceous pyroclastic flows). Beyond the 1964 deposits the plain is covered by heavy forest. Along the southern foot of the volcano, 17–22 km from the crater, the plain is bounded by a broad arc of large hills. These hills have been described as the end moraine of the last glaciation (Menyailov 1955) or as an ancient directed blast deposit (Gorshkov and Dubik 1970; Melekestsev et al. 1991). Our study has shown that the hills are large hummocks of the debris-avalanche deposit that resulted from the oldest and largest failure of the Old Shiveluch edifice and development of its horseshoe-shaped caldera.

The plain descending from the caldera breach is underlain by a sequence of volcanoclastic flowage deposits of Holocene age – pyroclastic flows, surges, lahars and debris avalanches, which accompanied the formation and periodic destruction of Young Shiveluch. To the east, north and west their distribution was confined by the high scarp of the caldera wall. The flowage deposits are interbedded with palaeosols and multiple layers of fallout deposits, most of which were produced by Young Shiveluch volcano; some tephra layers represent the distal ash from other Kamchatkan volcanoes. The fallout deposits derived from Young Shiveluch are represented by pumice, ash and lapilli of plinian eruptions: approximately 60 tephra layers have been identified, some as thick as 1 m.

Stratigraphy of the southern slopes of Shiveluch and determination of ages of the avalanches

Debris-avalanche deposits with C^{14} ages approximately 10,000, 5700, 3700, 2600, 1600, 1000 and 600 BP, and 1964 AD, were found on the southern slopes of Shiveluch volcano (Fig. 3). The oldest of these originated from the failure of the Old Shiveluch edifice, and the other seven are related to the failures of Young Shiveluch dome complexes.

Determination of age

The precise age of the Old Shiveluch debris avalanche is unknown. The only exposure of lower contact of the avalanche deposit is in a valley of Sukhoi Il'chinet's river, but the age of the underlying material is not known (Fig. 2). Inside the avalanche deposit no organic material has been found that is suitable for C^{14} dating. Mel-

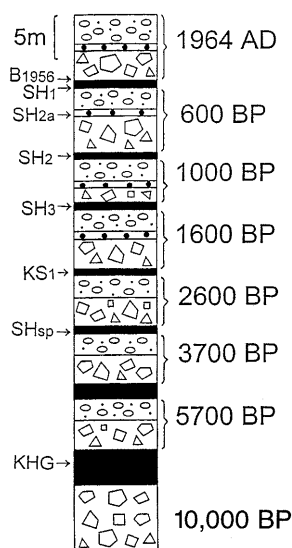


Fig. 3 Generalised composite stratigraphic section of the southern foot of Shiveluch volcano showing avalanche-eruptive units – deposits of debris avalanches and accompanying eruptions. Pyroclastic deposits unrelated to failures and palaeosols are shown as black areas. For complete legend see Fig. 5. Indices to the left of the column show the positions of fallout layers that were used for dating the avalanches (see text for details)

Melekestsev et al. (1974) estimated its age as 30,000 BP from indirect geological data. We consider this estimate as the oldest possible age. The oldest palaeosol above the avalanche deposit with enough humus for radiocarbon dating yields an age of approximately 8000–8500 C^{14} BP. This is considered as the young limit for the age of the avalanche. The failure probably occurred after the end of last glaciation at Kamchatka, approximately 10,000 BP (Melekestsev et al. 1991; Braitseva et al. 1995). Fluvioglacial deposits of this age, derived from a glacier on Shiveluch volcano, lie far to the south, but proximal hummocks of the avalanche were not eroded by the glacier or covered by glacial deposits. The youngest lava flow of the Old Shiveluch edifice was probably erupted after the glaciation but before the slope failure, because it has a fresh surface morphology unmodified by glaciers and its upper part is truncated by the caldera rim. Probably Old Shiveluch failed soon after the last glaciation when the climate was still cool, because the first soils that developed on the avalanche deposit have a very low content of humus. Thus, we nominally refer to the age of the Old Shiveluch debris avalanche as 10,000 BP.

Ages of the other six prehistoric debris avalanches of Young Shiveluch were determined mainly on the basis of correlation with interbedded fallout layers, which had been dated earlier by Braitseva et al. (1989, 1992, 1995) and by Ponomareva et al. (1998), using multiple radiocarbon dating of intercalated palaeosols. The following fallout layers (and associated ages) originated at Shiveluch: SH₁ (265 ± 18 BP), SH_{2a} (500–600 BP), SH₂ (965 ± 16 BP), SH₃ (1404 ± 27 BP), SH_{sp} (~3600 BP)

and distal ashfalls originated from Bezymianny (B₁₉₅₆, 1956 AD), Ksudach (KS₁, 1806 ± 16 BP) and Khangar volcanoes (KHG, 6957 ± 30 BP). These fall layers have distinctive features enabling them to be recognised easily in the field.

In some cases palaeosols directly underlying debris-avalanche deposits were also dated. Because the avalanche deposits were not dated directly, we rounded the ages of the failures to the nearest 100 years.

Each debris-avalanche deposit of Young Shiveluch is commonly covered by a set of pyroclastic layers represented by fallout and/or flow deposits (locally with corresponding ground surge and/or ash-cloud surge layers). These pyroclastic deposits lie directly above the debris-avalanche deposits, with no evidence of a hiatus between. We believe that these pyroclastic deposits were produced by explosive eruptions that accompanied the edifice failures. For convenience, we refer to each set of virtually contemporaneous deposits (avalanche + fall and/or flow) as an “avalanche-eruptive unit”. Deposits between avalanche-eruptive units are represented mostly by multiple palaeosols intercalated with fallout deposits, and, in places, with deposits of lahars and pyroclastic flows. Each set of these deposits is referred to as a “soil-pyroclastic sequence”.

The first avalanche-eruptive unit of Young Shiveluch was deposited above the KHG ashfall layer (6957 ± 30 BP), directly on soil with a C^{14} age of 5750 ± 300 BP. Thus, we consider the age of the slope failure as 5700 BP. The second avalanche-eruptive unit lies just below the distinctive dark grey, friable fallout layer SH_{sp} with an age of ~3600 BP and thus is referred to as a 3700-BP event. The third avalanche was dated as 2600 BP, because its underlying soil has an age of 2690 ± 70 BP. The fourth avalanche-eruptive unit was dated as 1600 BP, because it is mantled by 2 cm of soil, probably representing a few hundred years, and then by the SH₃ layer with an age of 1404 ± 27 BP. The fifth avalanche-eruptive unit was dated as 1000 BP, because it lies above the SH₃ layer and 2 cm of soil with an age of 930 ± 50 BP and is itself covered by the SH₂ fall layer with an age of 965 ± 16 BP. The sixth avalanche-eruptive unit overlies the SH₂ fall layer and is separated from it by 2 cm of soil. The avalanche is directly mantled by the SH_{2a} fall layer of the accompanying eruption, with an age previously estimated as 500–600 BP. Charcoal in a pyroclastic flow deposit of this avalanche-eruptive unit has been dated as 590 ± 100 BP. Thus, the failure took place around 600 BP. Possibly this event is reflected in a local aboriginal legend, reported by Krashennikov (1755): “Once upon a time, Shiveluch volcano was located far to the east coast, but then it was disturbed by ground squirrels, digging their holes in the volcanic foot and thus the volcano was forced to run away to the place of its present location. When Shiveluch was running it left two footprints – the lakes 25 km to the southwest from the volcano”. If the legend is connected with any real volcanic event, the best candidate may be the avalanche

at 600 BP, because deposition of the debris avalanche caused the formation of the two lakes. When Krasninnikov traveled in Kamchatka, less than 400 years had passed after this failure, and oral traditions of local tribes could have “remembered” the event.

The youngest and seventh avalanche-eruptive unit was deposited during the 1964 AD eruption of the volcano (Belousov 1995). Its deposit overlies the 1-cm-thick distal grey ashfall layer of the 1956 Bezymianny eruption (Gorshkov 1959).

When we started our study of Shiveluch volcano, we supposed that there was also a slope failure of the volcano in 1854 AD. We followed the statements of Gorshkov and Dubik (1970), which classified the 1854 eruption as a directed blast, and Siebert (1984), who mentioned a possible failure in 1854. Support for these conclusions included a description of the eruption (Krahmalev 1880) and the horseshoe-shaped morphology of the 1854 crater. Krahmalev wrote that “Shiveluch volcano had such a strong eruption in 1854 that a half of it was destroyed, huge stones devastated all forest on the foot of the volcano and the ice covering the Kamchatka river was broken into pieces”. The fallout deposit of the 1854 eruption lies north from the volcano (M.M. Pevzner, pers. commun.; Ponomareva et al. 1998). Despite these explanations, we did not find an 1854 avalanche deposit, although the 1964 deposits are sufficiently dissected by erosion to expose the underlying deposits. Moreover, we also did not find any flowage deposits of a similar age that could have devastated the forest in 1854.

A possible explanation is that in 1854 there was no slope failure but a strong explosive eruption that destroyed the old intracrater dome complex and strongly modified the old (probably 600 BP) horseshoe-shaped crater. The forest might have been damaged by block-and-ash flows and lahars that resulted from pyroclast-induced melting of snow (the eruption occurred in winter). These deposits were emplaced in river valleys and later either completely eroded and/or deeply buried under the 1964 deposits. An eruption with a similar scenario occurred at Shiveluch on 22 April 1993 (Firstov et al. 1995).

Stratigraphy

The plain descending from the avalanche caldera is dissected along its western boundary by the deep canyons of Baidarnaya and Kamenskaya rivers and along its eastern boundary by the Kabeku river (Fig. 2). Deposits of prehistoric debris avalanches were studied mostly along these canyons and tributaries, which have good continuous outcrops. The valley of the Kabeku river exposes the oldest avalanche deposits of the southern flank, those of 10,000, 5700, 3700 and 600 BP, as well as 1964 AD (Fig. 4). The valleys of Baidarnaya and Kamenskaya rivers expose the youngest avalanches: 3700, 2600, 1600, 1000 and 600 BP, and 1964 AD (Fig. 5). The

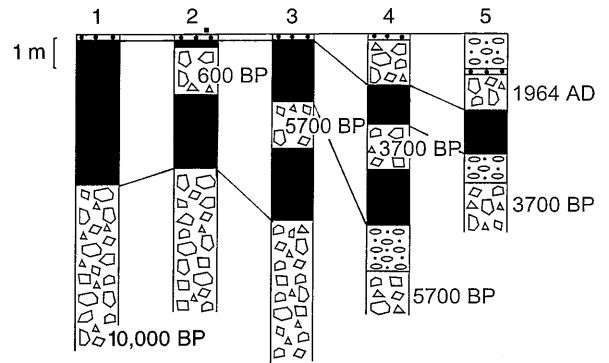


Fig. 4 Generalised stratigraphic sections of avalanche-eruptive units at the southeastern foot of Shiveluch volcano along valley of Kabeku river. Pyroclastic deposits unrelated to failures and palaeosols are shown as black areas. Location of sections at Fig. 2. For complete legend see Fig. 5

oldest part of the section (10,000–3700 BP) is described in detail from the Kabeku valley, and the rest (<3700 BP) from the Baidarnaya and Kamenskaya valleys. In the valley of Sukhoi Il'chinets river only the 10,000 BP avalanche deposit is exposed. No deposits of younger debris avalanches were found. Outcrops are very scarce along the other rivers along the southern foot of Shiveluch. The deposit of the 1964 debris avalanche is not vegetated and was studied in many places on its surface and in innumerable shallow gullies.

Kabeku river

The Old Shiveluch avalanche deposit (10,000 BP) is exposed in many outcrops along the valley of Kabeku river (Fig. 4, sections 1, 2, 3) where it crosses the aval-

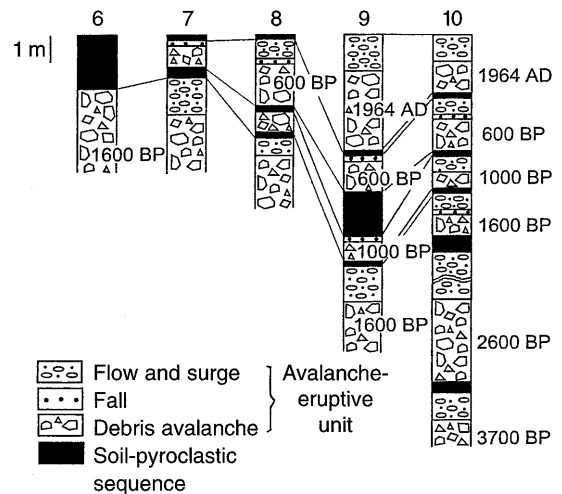


Fig. 5 Generalised stratigraphic sections of avalanche-eruptive units at the southwestern foot of Shiveluch volcano along valleys of Baidarnaya and Kamenskaya rivers. Pyroclastic deposits unrelated to failures and palaeosols are shown as black areas. For location of sections see Fig. 2

anche hummocks 14–20 km from the crater (Fig. 2). The maximum visible thickness of the avalanche in Kabeku river is approximately 30 m, but its basal contact is not exposed. No deposits were found along the upper contact of the avalanche that could represent pyroclastic deposits of an eruption accompanying this failure. At a distance of 20 km from the crater the avalanche deposit is mantled by a soil-pyroclastic sequence 5–6 m thick (Fig. 6).

Approximately 14 km from the crater, the section is wedged apart by four more debris avalanches: 5700, 3700 and 600 BP, and 1964 AD. The frontal parts of these avalanches were here channeled between large hummocks of the 10,000-BP avalanche, forming a complicated system of overlapping avalanche tongues of different ages separated by palaeosols and pyroclasts.

The 5700-BP avalanche appears in the valley of Kabeku river 14.1 km from the crater (Fig. 4, section 3). It is separated from the Old Shiveluch avalanche by a soil-pyroclastic sequence 2.5 m thick. The distribution of pyroclastic layers in the section shows that, after the 10,000-BP failure, the explosive eruptions (mostly plinian) of Young Shiveluch were very frequent but after approximately 7000 BP became rare. The 5700-BP avalanche lies directly on a palaeosol 15 cm thick. Thus, in the centuries before this failure, Shiveluch could have experienced either a long period of dormancy (or a period when explosive activity was too weak to be recorded in palaeosol) and/or a period of quiet extrusion of volcanic domes. The visible thickness of the 5700-BP avalanche deposit is 1–5 m. Approximately 14 km from the volcano, a 2- to 3-m-thick pumiceous pyroclastic flow, produced by the eruption that immediately followed the slope failure, lies along the upper contact of the avalanche deposit (Fig. 4, section 4).

The 3700-BP avalanche deposit crops out in the left tributary of Kabeku river 13–13.6 km from the crater

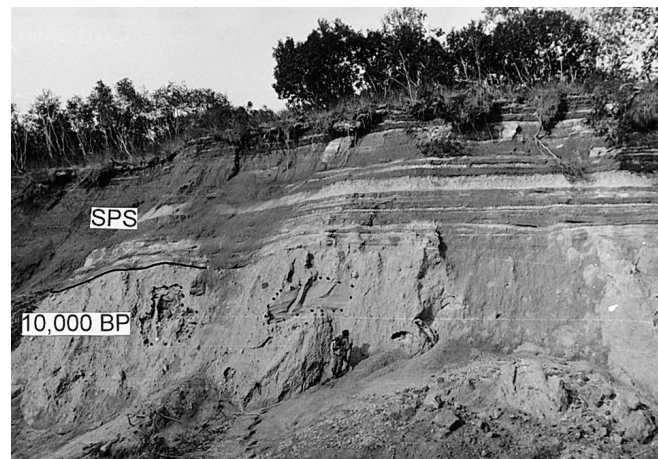


Fig. 6 The oldest (10,000 BP) debris-avalanche deposit of Shiveluch volcano (Kabeku river, section 1, Figs. 2, 4). Note two debris avalanche blocks in the middle part of the avalanche. The avalanche deposit is covered by soil-pyroclastic sequence (SPS), i.e. intercalated layers of fallout deposits (*light*) and palaeosols (*dark*). Person for scale

(Fig. 4, sections 4, 5). It is separated from the 5700-BP avalanche deposit by a 2- to 3-m-thick soil-pyroclastic sequence. Distribution of the pyroclastic layers in the sequence shows that, shortly after the 5700-BP event at Shiveluch, several plinian eruptions occurred. Then explosive activity declined for several centuries before resuming again. For several centuries preceding the 3700-BP failure, strong explosive eruptions (mostly plinian) were frequent. The 3700-BP avalanche deposit lies directly on thin palaeosol. The thickness of the avalanche deposit is 3 m, and it is covered by a pumiceous pyroclastic flow 1 m thick that immediately followed the failure.

The first tongues of the 600-BP avalanche deposit appear in the valley of Kabeku river 14.5 km from the crater (Fig. 4, section 2). Here this avalanche, without any deposits of an accompanying eruption, overlies the 10,000-BP avalanche deposit and a soil-pyroclastic sequence approximately 3 m thick.

The 1964-AD avalanche deposit extends 14 km from the crater, where it overlies a soil-pyroclastic sequence 1.5 m thick above the 3700-BP avalanche deposit. The 1964 avalanche deposit is covered here by a complete section of deposits of its accompanying eruption: a fine-grained olive-grey lithic ash 4–8 cm thick with abundant accretionary lapilli, plinian fallout pumice up to 20 cm thick, and pumiceous pyroclastic flow deposits 1–2 m thick (Fig. 4, sections 4, 5).

Baidarnaya and Kamenskaya river

Canyons of the Baidarnaya and Kamenskaya rivers are parallel and closely spaced and expose a similar stratigraphy. The canyon of the Baidarnaya river is deeper and exposes the older avalanche deposits, 3700 and 2600 BP. The canyon of the Kamenskaya river is more convenient for the investigation of the upper portion of the section, 1600, 1000 and 600 BP, and 1964 AD units (Fig. 7).

In the deepest part of Baidarnaya canyon 11 km from the crater, the river forms a small waterfall over a 3-m pile of large blocks of red andesite. These rocks are mantled successively by a pumiceous pyroclastic flow deposit 2 m thick, 2 mm of soil, a layer of pumice lapilli 38 cm thick and 3 cm of soil with an age of 2690 ± 70 BP (Fig. 5, section 10). Although the fallout layer SHsp (3650 BP) was not found here, the stratigraphic position of the rocks suggests that they are a facies of the 3700-BP avalanche deposit. Correlation of sections in Kabeku and Baidarnaya rivers shows that, between the 3700- and the 2600-BP avalanche, the explosive activity of the volcano was weak. But obviously the volcano was not dormant, because the edifice had accumulated at least 1 km^3 of rocks represented by the 2600-BP failure. Probably during that period the volcano experienced nonexplosive extrusion of lava domes.

The 2600-BP avalanche lies directly above the 2690 ± 70 BP soil (Fig. 5, section 10). The avalanche is



Fig. 7 Four avalanche units (1600 BP, 1000 BP, 600 BP and 1964 AD) exposed in canyon wall of the Kamenskaya river (section 9, Figs. 2, 5). Arrow points to person for scale

5 m thick and covered by a 20-m-thick pumiceous pyroclastic flow deposit from an eruption immediately after the failure. The distribution of pyroclastic layers in the soil-pyroclastic sequence above the avalanche deposit shows that, after the 2600-BP failure, Shiveluch volcano experienced several plinian eruptions, but then, several centuries before the next (1600 BP) failure, its explosive activity was weak. The 2600-BP avalanche is exposed only in this outcrop. Both upstream and downstream the layer descends below the base of the canyon under younger deposits. In the high cliff above, four avalanches are visible: 1600, 1000 and 600 BP, and 1964 AD (Fig. 5, section 10).

In the Kamenskaya river the 1600-BP avalanche deposit, 3–10 m thick, forms the lowest part of the section. In its distal zone, 19–20 km from the crater, it is the only exposed avalanche deposit (Fig. 5, section 6). There are no deposits of an eruption that accompanied the failure, and the avalanche is covered by the soil-pyroclastic sequence 2–3 m thick. But at distances <19 km from the crater, the avalanche is mantled by thin fine-grained ash fall and a 0.5 to 3-m-thick pyroclastic flow deposit of an eruption immediately after the failure (Fig. 5, sections 7, 8, 9, 10). Between the 1600-BP failure and next (1000 BP) avalanche, Shiveluch volcano produced one strong plinian eruption that deposited the SH₃ fallout layer.

The 1000-BP avalanche deposit, 0.5–2 m thick, crops out <16 km from the crater (Fig. 5, section 8). It lies directly on soil 1 cm thick. Deposits representing the accompanying eruption occur <13 km from the crater, with 2–10 cm of pink ashfall covered by 15 cm of grey pumice lapilli overlain by pyroclastic surge and/or flow deposits up to 10 m thick (Fig. 5, sections 9, 10). The 1000-BP avalanche-eruptive unit is overlain by 0.5 cm of soil, 5–10 cm of airfall, 1 cm of soil, 20–30 cm of pumice fall (SH₂ layer), 1 cm of soil and the next, 600-BP avalanche unit (Fig. 8).

The 600-BP avalanche moved farther than the 1000-BP avalanche, to a distance approximately 19 km from the crater (Fig. 5, sections 7, 8, 9, 10). It has a thickness

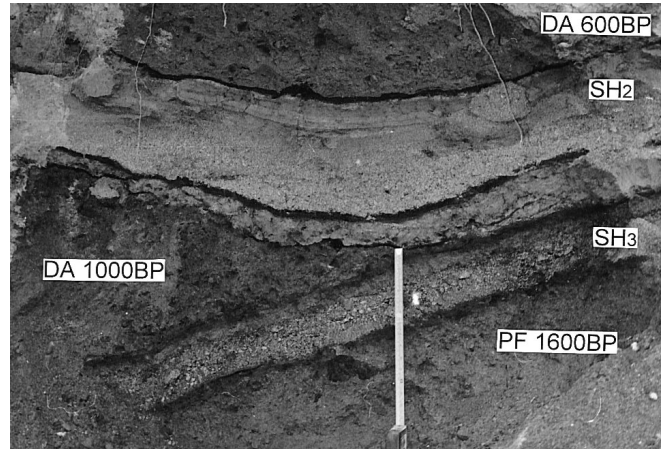


Fig. 8 Wedging of 1000-BP debris-avalanche deposit between 600- and 1600-BP avalanches and associated pyroclastic flow deposits. Valley of Kamenskaya river (section 8, Figs. 2, 5). DA and PF debris avalanche and pyroclastic flow deposits, respectively. SH₂ and SH₃ are fallout layers of plinian eruptions of Young Shiveluch that were used for correlation of the avalanches. Note that debris-avalanche deposits lie directly on palaeosols (black), which were not disturbed by emplacement of the avalanches. Scale is approximately 40 cm long

up to 10 m. Pink ashfall (up to 5 cm), grey pumice fall (SH_{2a}, up to 10 cm) and a pumiceous pyroclastic flow (up to 20 m) overlies the 600-BP avalanche and are the deposits of an eruption that immediately followed the failure. The 600-BP avalanche lies directly on 40 cm of the soil-pyroclastic sequence.

The 1964-AD avalanche extended 12–13 km down the valleys of Kamenskaya and Baidarnaya rivers. The deposit is as much as 10 m thick and overlies 10–20 cm of the soil-pyroclastic sequence above the 600-BP avalanche deposit. Here the 1964-AD avalanche deposit is covered by pumiceous pyroclastic flows of the eruption that immediately followed the failure (Belousov 1995). The flow deposit is as much as 50 m thick in channels but is commonly 2–10 m thick.

Material composing the debris-avalanche deposits

Most debris-avalanche deposits of Shiveluch volcano are similar in composition, structure, texture, grain size and general appearance in outcrops. The only exception is the avalanche of 1000 BP, which in most outcrops has a distinctive greenish colour, due to its origin from hydrothermally altered and probably water-saturated source rocks. It also is unusually thin in places, down to 20 cm.

The predominant material of all the avalanches is represented by block facies (terminology after Glicken 1986, 1991, 1998), characterised by sharp heterogeneity of constituent material as a result of incomplete mixing. Block facies is composed of “blocks” – irregular domains or lenses of strongly fragmented rocks from domes, lava flows, pyroclastic and talus layers, etc.,

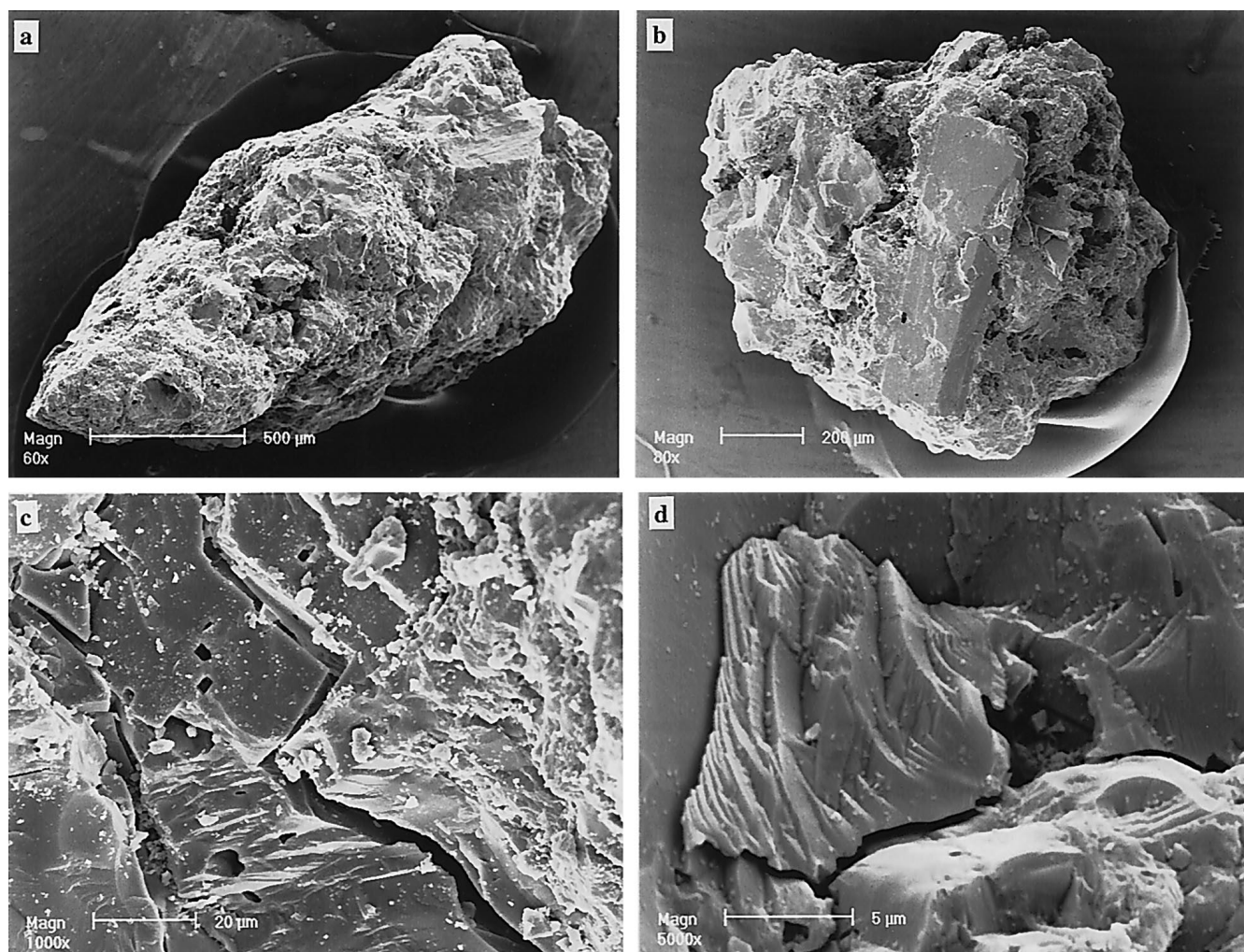
which originally composed the failed volcanic edifice. Dimensions of avalanche blocks are commonly 1–100 m but can be smaller or larger. The rocks are mostly andesite and, in the 10,000-BP avalanche deposit, also basaltic andesite. The degree of fragmentation of the rocks is commonly high, producing a sandy matrix, but there are also avalanche blocks composed of only slightly fractured massive lava.

Individual avalanche blocks have different colours (red, blue, yellow, grey, black, etc.), which depend on composition, degree of oxidation and hydrothermal alteration of source rocks. Strongly altered rocks are rare, except for those in the 1000-BP avalanche deposit. Blocks touch one another along irregular contacts, which are usually sharp but locally can appear diffuse. Irregular blocks of different dimensions and contrasting colours form a peculiar patchwork pattern in outcrops that is easily recognisable in the field. In many cases the avalanche blocks are strongly stretched in the direction of avalanche motion, and some blocks resemble discontinuous deformed layers. The fabric inside the avalanche blocks is generally massive and matrix supported, but some very poorly fragmented blocks have clast-supported fabric. Rock clasts usually have a

blocky angular shape and are petrographically identical to the surrounding matrix. Most clasts are roughly equant or slightly elongated, and larger clasts are commonly broken by several intersecting cracks and multiple microcracks, which allow them to split easily by hand. The block facies is composed of subrounded and/or heterolithological clasts, if the source material were pyroclastic or talus deposits.

Sand-sized particles of block facies are equant or slightly elongated with angular blocky morphology, and their surfaces are irregular with multiple corners (Fig. 9a,b). Surfaces of sand-sized particles show features similar to those recognised in the Mount St. Helens debris-avalanche deposit by Komorowski et al. (1991), namely microcracks and hackly surfaces (Figs. 9c,d). In the groundmass the microcracks have a chaotic orientation, but in crystals they are frequently controlled by crystallographic directions. We suspect that microcracks were formed not only by shear asso-

Fig. 9 SEM photomicrographs of **a,b** sand-sized particles from the 1964 debris avalanche and characteristic details of their surfaces: **c** microcracks and **d** hackly surfaces



ciated with slope failure but also by rapid unloading of lithostatic pressure during slope failure. Hackly surfaces possibly were formed by splitting of larger clasts across chaotically microfractured media.

“Mixed facies” material is represented by a comparatively homogeneous dark brownish-grey mixture of different pulverised rocks of the volcanic edifice, commonly with material entrained from the underlying surface. The tint of the mixture can be different, depending on the colour of the most abundant rock type. Tiny rounded or stretched inclusions of block facies, and unconsolidated pieces of underlying deposits (soil, old pyroclastic, debris alluvium) – together with uncharred wood fragments – are chaotically incorporated in this matrix. Mixed facies is rare in the interior of debris-avalanche deposits of Shiveluch but can be found in small amounts along the outer boundaries of the avalanches. A basal contact variety of the mixed facies, with a thickness up to 1 m (usually 5–20 cm), is a common feature of Young Shiveluch debris-avalanche deposits (Fig. 10). It probably represents the basal shear zone of the avalanches. The upper boundary of the shear layer is sharp but generally irregular in form, with bulbs and finger dikes of mixed facies penetrating upward inside the block facies, indicating its mobility.

In some places along the frontal boundary of the avalanches are ramparts of displaced underlying deposits. An especially large rampart was formed in front of the eastern part of the 1964 debris avalanche, where the underlying pyroclastic deposits up to several metres thick were scraped up and buckled in a band 6 km long and 1.5 km wide (Fig. 11), displaced several hundred metres from their original position. Similarly produced, displaced and deformed fluvio-lacustrine sediments containing avalanche blocks were described by Siebe et al. (1992) in front of the debris avalanche of Jocotitlan volcano, Mexico. Such formations can be separated as a



Fig. 10 Basal contact of 600-BP avalanche lying on pyroclastic flow deposit associated with deposition of fallout layer SH₂. Upper part of the avalanche is represented by block facies (BF); lower part of the avalanche is represented by mixed facies (MF) formed by intensive basal shear which also led to erosion of thin palaeosol above SH₂. Scale is approximately 25 cm long

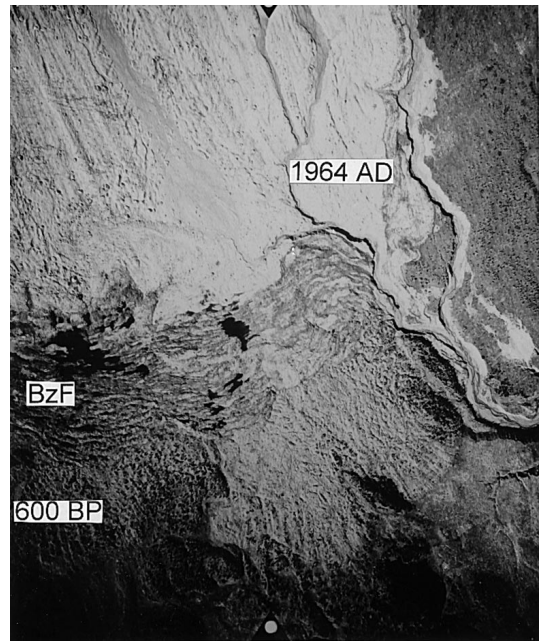


Fig. 11 Aerial photo of southeastern margins of 600-BP and 1964-AD debris-avalanche deposits. Valley of Kabeku river in right part of the photo. Area of sections 2–4 in Fig. 2, and of box A in Fig. 16. Surface of block facies of 1964-AD debris-avalanche deposit (light, in upper left quarter of the picture) is characterised mainly by quasi-parallel longitudinal furrows and ridges, on which are superimposed small conical hummocks. Surface of bulldozer facies (BzF) rampart of 1964-AD avalanche is represented by transverse folds with lakes in depressions (black). Hummocks of 1964-AD and 600-BP avalanches are very small in comparison with large hummocks of 10,000-BP avalanche, lower edge of photo

peculiar facies of debris-avalanche deposits – we term it “bulldozer facies.”

Juvenile material was not found in the debris-avalanche deposits. Contrary to the events on Bezymianny and Mount St. Helens, the failures of Shiveluch occurred before any rising batch of magma was intruded high into the volcanic edifice.

Granulometry

Grain-size distributions of 29 samples (eight from pre-historic avalanches, and 21 from 1964) were studied. Most samples had weights 0.5–1 kg each, but samples of very coarse-grained deposits were as much as 8 kg. The samples were subjected to standard dry-sieve analysis, with sieves from 5 to -6ϕ .

All but two samples represent block facies. We sampled only block facies that had originated from “solid rocks” (former domes and lava flows) on the failed edifice. Thus, their grain-size distributions reflect mostly processes of disaggregation or comminution during failure and transportation. Block facies that originated from previously disaggregated material of the failed edifice (former old pyroclasts and talus) were not sam-

pled, because their grain size was largely predetermined by their initial condition. Two samples were taken from the basal mixed facies.

All samples are classified as gravelly sand and sandy gravel with up to 15% admixture of silt and clay (Fig. 12; Table 1). Histograms of grain-size distribution (Fig. 13) of the deposits have several distinctive features:

1. The histograms commonly embrace the whole measured grain-size interval. Sometimes the coarsest fractions ($> -4 \phi$) are absent, but field observations show that in most cases this is the result of incomplete sampling. In larger volumes of the material, clasts of these sizes are actually present.
2. For many samples most size fractions display similar percentages, within 5–10%.
3. Histograms usually are polymodal. Modes: -3 , 2 and 4ϕ , and minimum -1ϕ , are the most common. The low between -1 and -2ϕ is seen in samples of block facies material at Mount St. Helens and Augustine volcanoes and may be typical for deposits of debris avalanches (Glicken 1998; Siebert et al. 1995).
4. Basal mixed facies is commonly finer grained than block facies.

Such diffuse, polymodal grain-size distributions result in poor sorting and a wide range of median diameters (Table 1). On a plot of median diameter vs sorting, most samples fall into the coarse-grained part of the axial zone of the pyroclastic-flow field of Walker (1971). Toward both the largest and the smallest median diameters, some improvement of sorting is common (Fig. 14). Because the avalanches contain boulder-sized clasts unsampled for sieve analyses (see below), the actual sorting of the deposits is poorer and median

Table 1 Granulometric characteristics of the debris-avalanche deposits of Shiveluch volcano. Number of samples in parentheses. Numbers on the first line are the lowest and highest values and on the second line the average value. Sorting and median diameter after Inman (1952). Gravel: 2 mm; sand: from -1ϕ to $+4 \phi$ (from 2 to 0.63 mm); silt + clay: $>4 \phi$ (>0.063 mm); $\phi = -\log_2$ diameter in millimetres

	Median diameter (ϕ)	Sorting (ϕ)	Gravel (%)	Sand (%)	Silt + clay (%)
1964 block facies (19)	-2.9–2.0 0	1.8–3.4 2.8	9.3–76.4 36.7	22.5–81.6 56.5	1.1–14.9 6.8
1964 mixed facies (2)	1.9–2.0 1.95	2.7–2.8 2.75	22.0–24.2 23.1	65.7–68.5 67.1	9.5–10.1 9.8
Prehistoric deposits (8)	-3.7–1.7 -0.1	2.9–3.4 3.1	23.4–71.1 40.2	26.5–66.8 53.4	2.4–11.8 6.4

diameter larger than points shown on the plot. Samples of mixed facies are among the most fine-grained deposits, probably as a result of additional shearing and entrainment of underlying soil.

Field observations show that the debris-avalanche deposits at Shiveluch are already strongly disaggregated near the source (3.5 km from the centre of crater)

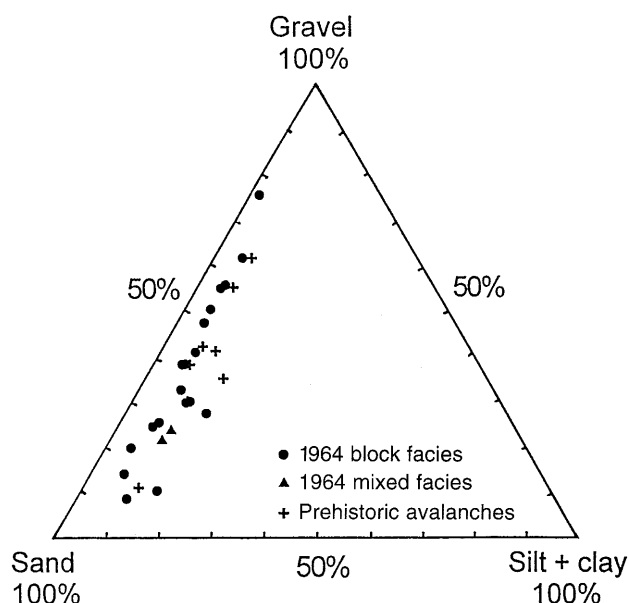


Fig. 12 Percentage of gravel (>2 mm), sand (from 2 to 0.063 mm), and silt + clay (<0.063 mm) in the debris-avalanche deposits of Shiveluch volcano

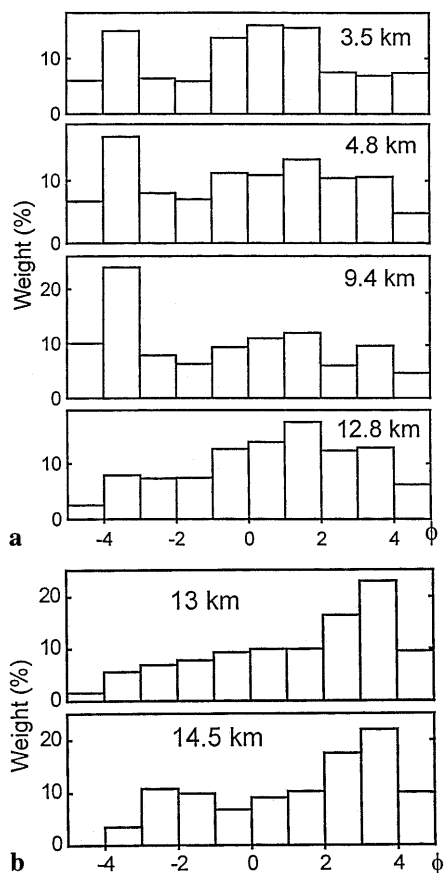


Fig. 13 Typical grain-size histograms of **a** block facies and **b** basal mixed facies of 1964 debris avalanche. Distance from the crater is indicated. Note that basal mixed facies is notably finer grained than block facies

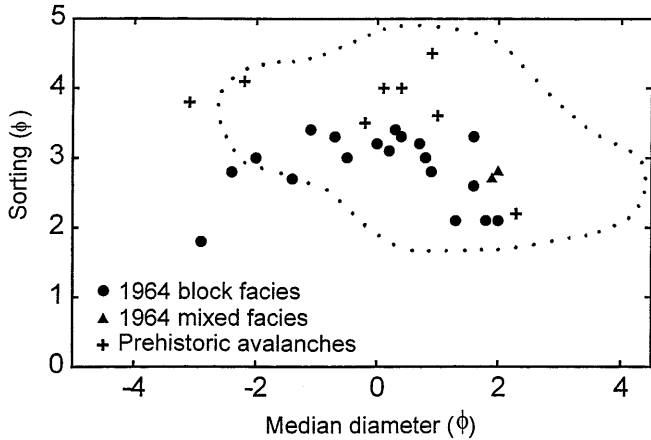


Fig. 14 Relationship between sorting and median diameter (Inman coefficients) for the debris-avalanche deposits of Shiveluch volcano. Dotted line shows field of pyroclastic flows after Walker (1971)

er). The same feature was reported for Mount St. Helens by Glicken (1986, 1998). To track changes of grain size with distance from the source, we took 11 samples of the 1964 deposits along the radial profile that coincides with the axial zone of the avalanche (Fig. 15). The profile starts 3.5 km away from the 1964 crater, at the base of the “steps” – huge slide blocks of the avalanche that stopped in the breach of the crater. The end of the profile is 13.7 km from the crater, near the front of the avalanche. To minimise the influence of different source-rock lithology, we sampled only block facies that originated from distinctive pink andesite of the former lava dome, one of the most abundant rock types in the avalanche. Although grain-size parameters along the profile are notably variable, there is some decrease in gravel content toward the front of the avalanche, compensated by a proportional increase of sand content. Silt + clay content is almost constant, with only a small increase toward the avalanche front. Accordingly, there is some decrease of median diameter and a slight improvement of sorting.

Two explanations can be proposed for the origin of the observed weak trends. One is that the frontal part of the avalanche is composed of material that, near the source and in the first moment of sliding, was already more strongly fragmented than the rest of the slide. For instance, it could represent the broken toe of the slide block, which formed the leading part of the avalanche. The second possible explanation is that, although most disaggregation occurred in the first moments of the failure, some additional fragmentation continued during debris-avalanche motion. Particles of all sizes in debris-avalanche deposits have multiple microfractures along which they can be easily split into fragments. Such splitting occurred during transportation of the avalanche material and caused the observed trends.

To characterise the coarsest fraction of the 1964 deposits, we calculated the average diameter of the ten

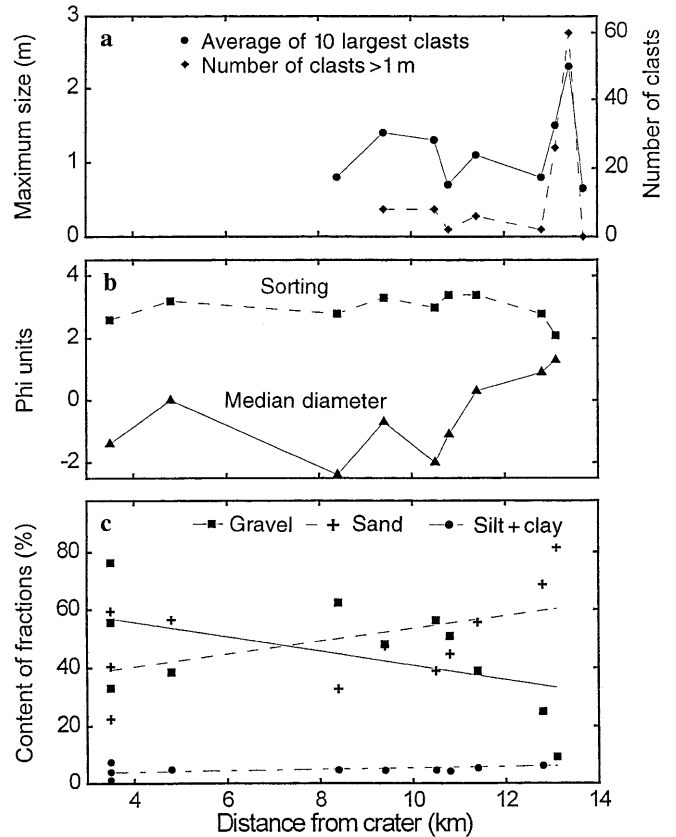


Fig. 15a–c Granulometric characteristics of block facies of 1964 debris-avalanche deposit vs distance from the volcano along the profile shown in Fig. 16. **a** Average size of ten largest clasts and number of clasts larger than 1 m measured on upper surface of the avalanche on area 100 m². **b** Sorting and median diameter (Inman coefficients). **c** Gravel (>2 mm), sand (from 2 to 0.063 mm) and silt + clay (<0.063 mm)

largest clasts and also recorded the number of clasts larger than 1 m per unit of area of the avalanche surface. The average of the ten largest clasts in a 100-m² area is from 0.7 up to 2.3 m, whereas the same measurement for 10,000-m² yields 1.6–3.6 m. The number of clasts more than 1 m across in an area of 100 m² is typically two to eight but sometimes as much as 60. The measured parameters show no clear trend with distance from the source (Fig. 15). Apparently, random fluctuations of values commonly coincide with the transition from one avalanche block to another and probably reflect local changes of mechanical properties of the rocks. For example, the largest value of the parameters at 13.4 km of the profile is due to the presence of very hard rocks in the avalanche.

Geometry and surface relief

In outcrops along walls of the river canyons, the debris-avalanche deposits of Young Shiveluch form semicontinuous layers with thicknesses around 1–10 m, and for

the Old Shiveluch avalanche, as much as 30 m. The frontal terminations of the avalanches are steep, generally several metres high, suggesting a significant yield strength of the material. There is no evidence that the downslope avalanches transformed into lahars. Beyond the frontal parts, thin fluvial deposits syndepositional to the avalanches were found in several cases but only in the main river valleys.

In plan view all the debris-avalanche deposits of Shiveluch volcano form broad fans that blanket one another. The avalanche boundary is clearly known only for the 1964 avalanche. The prehistoric avalanches are buried by different deposits and are heavily vegetated. Thus, the 10,000, 1600 and 600-BP avalanches could be mapped only approximately, using air photos (Fig. 2). First the positions of their frontal margins were determined in outcrops along Baydarnaya, Kamenskaya and Kabeku rivers. Then the margins were drawn by tracing breaks in slope above buried steep frontal boundaries of the avalanches. Discriminations between avalanches of different ages were made also on the basis of their different surface features (mostly dimensions and shape of hummocks). Because the avalanches of 5700, 3700 and 2600 BP are completely buried by thick younger deposits, and were found in few outcrops, their distribution is unknown.

The Old Shiveluch avalanche deposit occupies the largest area. Probably the frontal boundary of its distribution is marked by the band of large hummocks outlining a broad arc 15–23 km from the summit of Old Shiveluch. In the southwest part of the band, the hummocks form a projecting lobe 3 km wide, which spreads 35 km from the summit to the channel of the Kamchatka river. The elevation of the tip of the tongue is approximately 20 m a.s.l. The fall height of the avalanche (H) was at least 4 km and travel distance (L) = 35 km, so H/L is >0.11 . Along the outer boundary of the band of large hummocks is a break in slope 80–100 m high. Probably it corresponds approximately with the thickness (h) of the frontal part of the avalanche. The area covered by the deposit (S) is approximately 350 km², and the volume (V) is approximately 28–35 km³. If the pre-failure shape of Old Shiveluch was close to a regular cone, the maximum volume that could be removed by the failure is approximately 40 km³ (20% of the former edifice). The calculated volume of the avalanche is notably smaller. Thus, either the avalanche is thicker than supposed, or the pre-failure edifice had an irregular shape, possibly with deep canyons formed by recent glaciation, or perhaps thin avalanche material extends beyond the steep avalanche front (possibly in the form of avalanche-induced lahars).

Avalanches of Young Shiveluch are much smaller in scale than that of Old Shiveluch. The 1964 avalanche has the following characteristics: $H=2.3$ km, $L=16$ km, $H/L=0.14$, $S=98$ km² and $V=1.5$ km³ (approximately 15% of the pre-1964 Young Shiveluch edifice). Available data show that all prehistoric avalanches of Young Shiveluch were similar in scale to the 1964 avalanche.

Their characteristics have approximately the following limits: $H=1.5$ – 2.5 km, $L=11$ – 20 km, $H/L=0.12$ – 0.16 , $h=0.5$ – 10 m, $S=100$ – 150 km², $V=1$ – 2.5 km³.

Surface relief

Surface features can be observed for the avalanches of 10,000, 1600 and 600 BP, and 1964 AD. They display hummocky relief, typical for avalanches of volcanic origin (Ui 1983; Siebert 1984). For the prehistoric avalanche deposits only the distal parts are observed, although they too are partially obscured by younger deposits and heavy forest. The proximal parts of the prehistoric avalanche deposits are completely buried by younger deposits. The relief of the 1964 AD avalanche has excellent preservation and is available for observation on the complete surface, except for some proximal and medial areas covered by the 1964 pyroclastic flows.

Hummocks of the Old Shiveluch avalanche deposit are large, 10–130 m high with a base 0.2–2.5 km across, and slope angles up to 35°. The total number of hummocks higher than 10 m is approximately 100 (Fig. 2). Probably there are also smaller hummocks, masked by younger deposits and heavy forest. The highest hummocks are concentrated in the southwest part of the avalanche fan, where six of seven hummocks higher than 100 m are situated. Most of the hummocks are oval in plan view, with aspect ratio approximately 1:2. The axes of elongate hummocks have no apparent preferred orientation. The exposures along Kabeku river, which cut several hummocks, show that they are composed of typical block facies of the avalanche and have an internal structure similar to the structure between the hummocks.

Available data show that prehistoric avalanche deposits of Young Shiveluch have hummocky relief usually less than 10 m amplitude. Their relief in general is similar to that of the 1964-AD avalanche deposit.

Surface features of the 1964 avalanche deposit

The surface relief of the debris-avalanche deposit, together with its internal geological fabric, provide information about the processes of avalanche formation, emplacement and deceleration. These processes are ideally expressed in the 1964 avalanche, deposited in unchannelled conditions on a flat gentle slope (Fig. 16). We distinguish three classes of primary surface features:

1. Features resulting from incomplete disintegration of the failed part of the edifice
2. Features resulting from avalanche transportation (flowage processes)
3. Features resulting from avalanche deceleration

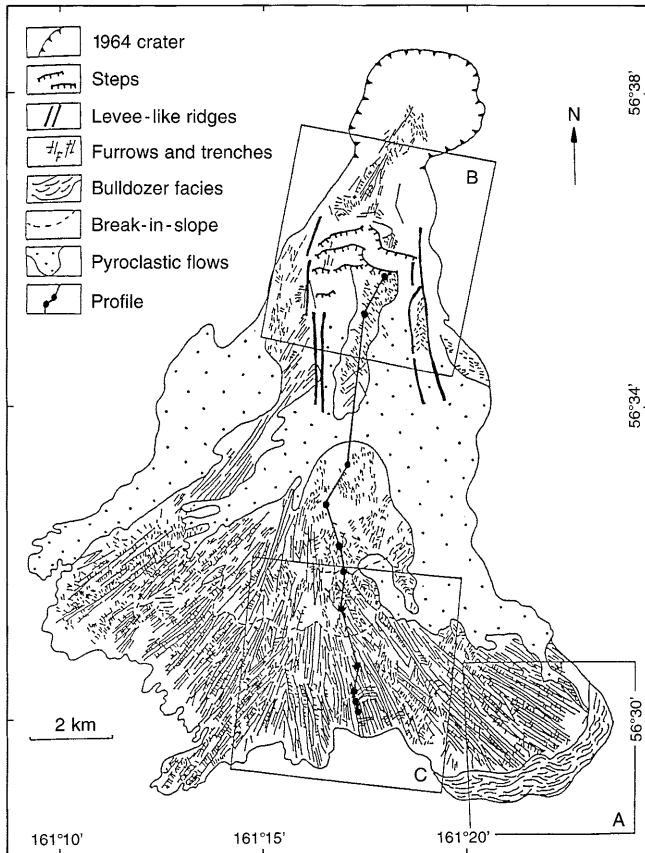


Fig. 16 Generalised map of surface features of 1964 debris avalanche based on aerial photos. Hummocks are too small to be shown. Boxes A, B, C are approximate areas shown on Figs. 11, 18, 20. Profile shows position of sampling points for grain-size analysis of Fig. 15

Features resulting from incomplete disintegration of the failed part of the edifice

The largest and most proximal surface features of the 1964 avalanche are three high scarps, in the breach of the horseshoe-shaped crater 2 km from the centre of the crater. The scarps parallel one another and are perpendicular to the direction of motion of the avalanche, resembling three giant steps (Figs. 16, 17, 18). In the scarps, the largest of which is up to 50 m high and 1.5 km long transverse to the avalanche movement, broken but relatively intact parts of failed edifice crop out. The upper surfaces of the steps are gently inclined toward the crater. The shape of the “steps”, their location and their internal structure suggest that they represent nearly intact parts of the pre-1964 dome complex, displaced several kilometres south from their original position. Just as at Mount St. Helens (Voight et al. 1981), the failure probably started as a retrogressive landslide with backward rotation of slide blocks. The unconstrained leading blocks were transformed into the debris avalanche, whereas the last slide blocks were



Fig. 17 Oblique aerial view of 1964 crater with the 1980–1981 dome inside. At foreground are two transverse scarps (“steps”), formed by the last slide blocks released in the 1964 avalanche, which stopped in the breach of crater

held up by the debris in front and soon began to decelerate.

This behaviour is not unique. Similar blocks are described for volcanoes Socompa, Chile (“toreva” blocks of Wadge et al. 1995) and Avachinsky, Kamchatka (Castellana et al. 1995). At Shiveluch volcano before 1964, in the location of the present “steps”, there was a distinctive large hill named Arbuzik (Menyailov 1955). It is possible that Arbuzik represented the most rearward, retrogressive slide block of the pre-1964 failure (probably 600 BP).

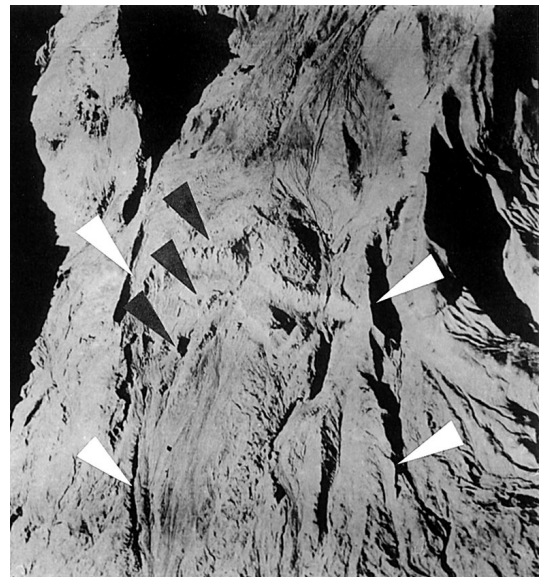


Fig. 18 Vertical aerial photo of a breach in 1964 horseshoe-shaped crater (box B in Fig. 16). The crater itself is beyond the upper edge of the picture. In the central part are three “steps” (black arrows) bounded by longitudinal levee-like ridges (white arrows)

The complete surface of the 1964 debris-avalanche deposit is dotted by innumerable small hummocks with nearly conical shape (referred to below as “conical hummocks”; Fig. 19). These hummocks are abundant on the deposits at all distances from the volcano and appear to be superimposed on all surface irregularities of larger scale. The hummocks are usually less than 10 m high (commonly 1–5 m) with a circular or oval base 0.5–2.5 m across. Slopes of the hummocks are usually 15–35°, comprising a talus apron covering a core of block facies. The talus aprons (and hence conical shape) were formed as a result of disintegration of irregular, gravitationally metastable projections of block facies at the surface of the debris avalanche. Comparison of photos taken shortly after the 1964 eruption (Gorshkov and Dubik 1970) with the present-day morphology shows that small talus aprons were formed during or immediately after avalanche emplacement and then gradually increased around the hummocks with time. In some places coherent block facies material emerges from the talus apron in the upper part of a hummock, with steep to vertical summit parts. The summits of conical hummocks are commonly pointed but can be irregular or flat (horizontal or inclined). The block-facies material inside each hummock is commonly represented by one rock type (one block), but hummocks containing more than one block are not rare. Nearby hummocks usually have a similar composition. In several places nearby hummocks composed of several rock types display similar stratigraphy. We infer that conical hummocks represent small brecciated pieces of the former volcanic edifice that were not completely disintegrated during emplacement of the debris avalanche.

Some of the conical hummocks are surrounded by circular depressions 1–6 m wide and up to 2 m deep. The origin of these depressions is not clear. Perhaps they were formed during or immediately after the cessation of avalanche motion, as intact hummocks sunk into loosened material of the mobile avalanche.

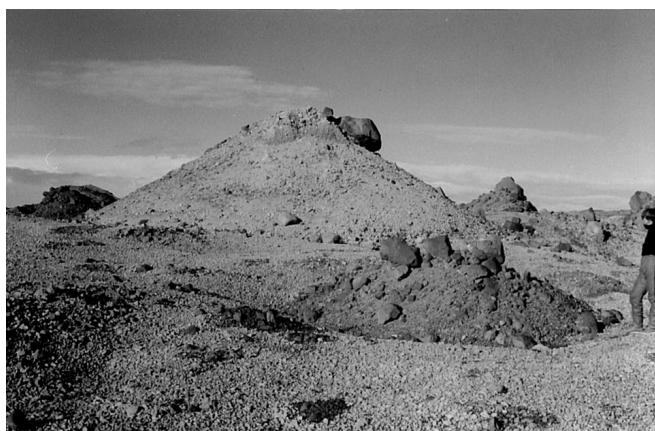


Fig. 19 Conical hummocks on surface of the 1964 debris-avalanche deposit. *Person* for scale

The number of conical hummocks per unit area is strongly variable. Hummocks can be separated by large, comparatively flat areas or can be closely spaced or even joined at their bases. Field observations show that the density and dimensions of conical hummocks depend neither on distance from the volcano nor on proximity to avalanche margins. If all rocks in a former edifice have uniform mechanical properties, a decrease of hummock heights with distance can be expected (Siebert 1984; Glicken 1991); thus, the farther from a source, the more its disintegration. But for strongly heterogeneous source rocks (as in the 1964 failure), the resultant surface of a debris-avalanche deposit resembles a mosaic of rocks with contrasting mechanical properties. The properties influence both the dimensions and density of hummocks and mask the effect of their progressive disintegration with distance.

Locally, the avalanche surface has few or no conical hummocks. In such areas large angular rock clasts are scattered on a sandy gravel substrate. Such areas apparently represent parts of the avalanche where complete disintegration of projecting hummocks (and hence of the failed edifice) occurred during motion of the avalanche. In these areas the maximum dimensions of clasts, and their concentrations per unit area, are different from one place to another over hundreds of metres, commonly corresponding with a change of the prevalent rock type in the area. The changes probably reflect the original edifice stratigraphy.

Features resulting from avalanche transportation

Contrary to the “disintegration features”, features resulting from avalanche transportation were produced from disintegrated material as a consequence of movement (flow) of the debris avalanche.

The “steps” in a breach of the 1964 crater are bounded by two parallel, longitudinal (aligned in the flow direction), levee-like ridges 10–30 m high and 2.5 km long (Figs. 16, 18). The ridges are composed of block facies and are interpreted as marginal levees, marking the boundary of avalanche flowage.

The medial and distal parts of the surface of the 1964 avalanche deposit have multiple, long, subparallel longitudinal furrows separated by ridges that generally have dimensions comparable to those of nearby furrows. The furrows form a distinctive, peculiar and “striated” pattern clearly visible on air photos (Figs. 11, 16, 20). The furrows are usually 1–30 m wide, 0.3–10 m deep, metres to kilometres long, and are oriented strictly in the direction of movement of the avalanche. In the medial part of the avalanche deposit, the furrows are less prominent than along the avalanche front. Furrows bifurcate toward the frontal boundary of the avalanche deposit, generally where avalanche lobes become broader.

The first impression is that the furrows are some kind of interior levee, but tracing of geological contacts



Fig. 20 Vertical aerial photo of surface of 1964 debris avalanche (box C in Fig. 16). Steep front of the avalanche deposit is in the lower part of the photo. Note longitudinal furrows and transverse trenches which “striate” the deposit surface

on the avalanche surface shows that there are no notable contact shifts where they are crossed by furrows. Thus, there was no significant relative movement of material among many neighbouring furrows. Typically the furrows continue to the front of the avalanche deposit. If the avalanche front was impeded by any obstacle, the furrows along the frontal boundary are strongly deformed or completely disintegrated, forming a hummocky surface. Hummocks formed as a result of furrow-ridge disintegration are notably elongate, or irregular in plan view, and have gentle slopes in comparison with conical hummocks. Longitudinal furrows similar to those described herein are visible on the surface of several other volcanic debris avalanches including So-compa, Chile (Wadge et al. 1995), Harimkotan, Kurile Islands and Taunshits, Kamchatka (A. Belousov and M. Belousova, unpublished data) and some large landslides of nonvolcanic origin on the Earth and Mars (Shaller 1991a, 1991b). Such furrows are produced by avalanche motion, probably during extensional strain of debris avalanche material with unusual rheology.

The frontal part of the 1964 debris-avalanche deposit was channelled in some places by depressions in the underlying surface. In former stream valleys, narrow tongues of avalanche material were formed, and lateral levees as high as 10 m were produced.

Features resulting from avalanche deceleration

Notable features of medial and distal parts of the avalanche surface are transverse graben-like trenches cutting the furrows and ridges at a highly oblique angle, usually 45–90° (Figs. 16, 20). The trenches are tens to hundreds of metres long and up to several metres wide and deep. They commonly form subparallel sets. Where the trenches are numerous, they commonly slice

the longitudinal ridges into short, hummock-like pieces. The trenches clearly represent extensional fissure-like structures, perhaps associated with longitudinal velocity gradients in the decelerating avalanche due to the medial portion having more drag than the frontal portion.

The surface of the bulldozer facies has multiple transverse undulating ridges, up to 10 m high, which in plan view are convex toward the avalanche front (Fig. 11). The ridges are clearly the surface expressions of folds and underlying imbricate shear zones in near-surface soils and tephra, formed by compressive forces applied to the substrate by the advancing but decelerating avalanche. The effect is pronounced near the avalanche snout at this particular location, because of local topography effects at a bend in the Kabeku river.

Discussion

Primary causes of edifice collapse

Evaluation of known cases of large-scale failures on volcanoes throughout the world (Voight et al. 1981, 1983; Ui 1983; Siebert 1984, 1996; Francis and Wells 1988; Moore et al. 1989; Siebe et al. 1992; Voight and Sousa 1994; Belousov 1995, 1996; Belousov and Belousova 1996) shows that failure can occur, given the right combination of circumstances, at almost any reasonably high volcanic edifice. Structural factors, such as steep dip slopes with interbedded fractured lava flows and unconsolidated pyroclastic materials, high water tables, extensive hydrothermal alteration in areas surrounding the central conduit, and abnormal pore-fluid pressures, are recognised as significant factors (Voight et al. 1981, 1983; Siebert 1984, 1996; Voight and Elsworth 1997). Most high volcanic edifices appear relatively weak in general, but relative weakness alone is insufficient for large-scale failure. Failures typically occur in association with some strong disturbance. If a disturbance is sufficiently strong, even a strong edifice can fail, whereas if disturbances are absent, a much weaker edifice can remain intact, though subject to gradual erosive processes.

What kinds of disturbances cause edifice collapse? Failures of Shiveluch and of other volcanoes show that many collapse events are strongly correlated with magmatic eruptions (Siebert 1984, 1996; Belousov and Belousova 1996; Voight and Elsworth 1997). Thus, disturbance of the edifice by some process that accompanies the magmatic eruption is a primary reason for most large-scale edifice failures. Large-scale failures accompanied by solely phreatic eruptions, or without any volcanic activity, appear less common, and their triggering mechanisms (such as tectonic earthquakes) are similar to those of nonvolcanic landslides.

The edifice of the Old Shiveluch volcano did not fail for tens of thousands of years despite its huge dimensions, steep slopes, the presence of a friable pyroclastic

sequence at its base, intensive volcanic activity and intrusion of multiple parallel dikes. Then, approximately 10,000 years ago, something changed. After the first giant failure of the stratocone, frequent smaller failures of the repeatedly active dome complex occurred. The rate of magma supply continued to be high, but frequent failures did not allow the volcano to recover its former shape and dimensions. The main change 10,000 years ago appears to have been the increase of SiO₂ content from approximately 55–56 to 60–62% (Dril 1988). The consequent increase in viscosity resulted in the appearance of lava domes rather than lava flows of long runout.

Highly viscous magma can build steeper volcanic edifices, obviously more favourable for collapse. In addition, and perhaps more importantly, highly viscous magma strongly disturbs the edifice as it ascends toward the surface. This disturbance is manifested in several ways, such as seismic deformation of the conduit and edifice, and degassing-induced seismicity. Degassing promotes crystallinity and further enhances bulk viscosity, resulting in non-linear pressure gradients and enhanced upper-conduit deformation. The bulk rock deformation and the higher water content of ascending silicious magmas can raise the pore-fluid pressure within the edifice by several mechanisms (Mori et al. 1989; Voight and Elsworth 1997) and thus favour slope failure.

All edifice failures of Young Shiveluch occurred when a new batch of volatile-rich magma ascended to a relatively high level (indicated by post-collapse plinian eruptions) but not within the edifice (indicated by lack of juvenile material in the avalanche, and by no lateral blasts). Similar conditions prevailed during the 1933-AD and 2000 ¹⁴C-BP failures of Harimkotan (Belousov and Belousova 1996), and probably the situation is common worldwide, as plinian eruptions in general are far more common than lateral blasts in association with edifice collapse. Thus, contrary to circumstances at Bezymianny and Mount St. Helens, strong shallow deformation and oversteeping of slopes by cryptodome intrusions were not the key factors for the Shiveluch failures. We believe that the most likely trigger for dome failure was the shaking produced by moderate-to-large volcanic earthquakes (M 4–6) at shallow depth under the edifice, perhaps in association with release of pressurised juvenile gas that raises pore fluid pressure in the edifice. The shaking produced from these shallow moderate earthquakes is much more severe than that from larger tectonic earthquakes at distances of 100 km or more.

Thus, the edifice failures of Shiveluch reflected a balance between properties of the edifice, which determine its general stability (dimensions, altitude, shape, internal structure, mechanical properties of rocks), and destabilising disturbances produced by the shallow intrusion of volatile-rich viscous magma under the edifice. The instability was a consequence of the high viscosity and high water content of the ascending magma,

with the most likely trigger mechanism a shallow-focus large volcanic earthquake and/or rapid enhancement of fluid pressure in the edifice resulting from degassing magma injected to high levels in the crust.

Frequency, direction of failures and future activity of Shiveluch volcano

The high frequency of failures of Young Shiveluch is related to its instability due to eruptions of very viscous magma and to its extremely high rate of magma supply, estimated by Melekestsev et al. (1991) as 36×10^6 tons/year, which allows rapid reconstruction of the edifice after each failure. Other volcanoes with known multiple failures, e.g. Augustine (Siebert et al. 1995), Colima (Komorowski et al. 1993) and Harimkotan (Belousov and Belousova 1996), also erupt very viscous magma and have a high rate of its supply.

The interval between the failures of Shiveluch volcano decreased with time. The first and longest interval, approximately 4300 years was needed for the construction of the Young Shiveluch edifice, following the severe destruction of Old Shiveluch by the enormous 10,000-BP failure. The recurrence intervals following the first failure of Young Shiveluch were much less than this interval, because only a fraction of the edifice was destroyed in subsequent events and needed rebuilding. The reason for the subsequent shortening of recurrence intervals is not known but could reflect an increase in the rate of magma supply.

All the failures of Shiveluch volcano occurred in the same, southern direction. We do not know what determined the direction of the first failure, but the younger failures were definitely influenced by that direction. The high walls of the avalanche caldera of Old Shiveluch confined the lava flows and talus produced by Young Shiveluch. As a result, the southern slope of Young Shiveluch was steeper, longer, less constrained and more favourable for failures than other directions.

The history of Young Shiveluch indicates that, during the last several thousand years, periods of vertical explosive eruptions and formation of lava domes were followed by repeated destruction by edifice failures. Explosive eruptions, which accompany episodes of dome growth, can also destroy the domes and thus delay the time of the next failure (as probably occurred in 1854 and also in 1993 (A. Belousov and M. Belousova, unpublished data).

Since the last failure of the volcano in 1964, a new dome with a volume of 0.2 km³ has formed in the crater (Firstov et al. 1995; Dvigalo 1995). The time of the next failure will depend on the rate of reconstruction of the edifice to a critical size and on the development of a destabilising disturbance. If the process is similar to that of previous millennia, the failure should occur no later than around 2350–2550 AD. The similarity of all failures of Young Shiveluch suggests that the size of the

future failure, and the style of its accompanying eruption, will be similar to that in 1964 (Belousov 1995). Probably the volcano will continue to operate in such a regime until a strong change occurs in its magmatic system or edifice morphology. For example, if SiO₂ notably decreases, episodic dome growth and failure may be discontinued, and the volcano may resurrect the form of Old Shiveluch. A strong perturbation of the plumbing system and the morphology of the volcano could also be produced by a caldera-forming eruption, which is feasible because the volcano has a large shallow chamber of silica-rich magma.

Formation and emplacement of debris avalanches

The following description represents the “averaged portrait” of edifice failure of Shiveluch volcano. It is drawn mostly from the 1964 avalanche but is thought to be representative for other avalanches of Young Shiveluch. With less confidence it describes the Old Shiveluch avalanche, because its volume is one order of magnitude higher and many important details of the deposit are not known (character of basal layers, style of accompanying eruption).

Each failure of Shiveluch probably starts as a seismically triggered retrogressive landslide, with propagation of successive slide blocks rearward and with backward rotation of individual slide blocks. Soon after the onset of sliding, the leading blocks transform into a debris avalanche, but the last slide blocks sustain less disaggregation, decelerate soon after the beginning of their motion and come to rest to form “steps” in the breach of the newly formed horseshoe-shaped crater. Although much of the disintegration of the leading block occurs at the beginning, small pieces of material on its surface are not completely disintegrated and form conical hummocks.

The avalanche propagates as a laminar plug flow, where the plug represents a transient wave of debris with high yield strength, gliding on a thin layer of mixed facies in the avalanche base where most of the shear strain is concentrated. During laterally unconfined motion on the open plain, the plug spreads radially, forming a thinning fan-shaped body of the block-facies-dominated debris-avalanche deposit. Such inhomogeneous radial extension of the avalanche body forms slightly diverging (but locally quasi-parallel) longitudinal furrows on the surface of the avalanche and leads to elongation of the debris avalanche blocks in the direction of movement. Near the end of its motion, sets of transverse quasi-parallel fissure-like trenches form on the surface of avalanche, reflecting localised longitudinal extension gradients that increased toward the distal end of the avalanche. The avalanche comes to rest more or less en masse. The trenches on the surface of the 1964 deposit suggest, however, that stoppage may be initiated from the interior of the avalanche body, leading to inhomogeneous extension of the distal

avalanche block-facies plug away from the rest of the avalanche.

Conclusion

The following conclusions were reached as a result of this study:

1. Large scale failures occurred at least eight times during the history of Shiveluch volcano. The volcano was stable in the Late Pleistocene when a large cone was formed and became unstable in the Holocene, in particular when a much smaller edifice that formed within the large collapse caldera of Old Shiveluch began to generate frequent debris avalanches. The transition in behaviour was connected with an abrupt compositional change to more viscous and volatile-rich magma.
2. The immediate cause of the failures was disturbance of the volcanic edifice by ascent of a batch of viscous, water-rich magma to shallow levels. In all cases the failures occurred before magma intruded into the edifice, thus suggesting that the trigger mechanism was indirectly associated with the rising magma. The most likely destabilising mechanisms involved shaking by a moderate or large volcanic earthquake and/or increased edifice pore pressure due to pressurised gas release from the ascending magma.
3. The “typical” edifice failure includes retrogressive collapse, backward rotation of slide blocks and transformation of the leading blocks into a debris avalanche. The last-released slide blocks come to rest relatively quickly, but the debris avalanche can be emplaced to distances exceeding 15 km. The avalanche resembles a transient wave of debris with high yield strength gliding on a thin basal layer of mixed facies.
4. All failures of Young Shiveluch were accompanied by explosive eruptions that followed a similar scenario. The edifice failure and generation of a debris avalanche were the first events, followed by a depressurisation-induced plinian eruption generally with some pyroclastic flows resulting from partial collapse of the fountain. During some failures a phreatic explosion occurred prior to the plinian eruption, probably caused by unloading of the hydrothermal system. The eruptions were of moderate size, and they were ordinary events in the history of the volcano, similar to numerous others that occurred without edifice collapse. No evidence for directed blasts was found, because failure preceded ascent of magma into the edifice.

Postscript

A paper by Ponomareva et al. (1998) on debris avalanches and the Holocene history of Shiveluch appeared

in *Bulletin of Volcanology* after our paper had been submitted. Their paper complements ours in providing detailed descriptions of tephrochronology and radiocarbon dating. In addition, their paper suggests overlapping deposits of at least 13 large Holocene debris avalanches, including in that number the debris avalanches described by Belousova (1994, 1996), Belousova and Belousov (1994a, 1994b) and also those discussed in our paper. However, we disagree with the significance attached to their other proposed avalanche deposits, with approximate ages 1450, 1700, 1850, 1900, 3100, 4000 and 5500 BP (their avalanches II, III, V, VII–IX, XI). Their avalanches VII and XI concern relatively small mass movements, probably related to localised failures of the west flank domes. The correlation of these deposits to thin coarse-grained deposits south of the main caldera rim of Old Shiveluch seems suspect. In general, their descriptions of the avalanche deposits are sparse, and some are not described. However, the descriptions provided (“subrounded” clasts, transitions to muddy material, etc.), and the restricted nature of the outcrops, suggest to us that many of these deposits represent lahars, block-and-ash flows or small landslides, rather than large Holocene debris avalanches composed of block-facies material. We have examined the valley outcrops they described. Thus, although we do not preclude the possibility of some large dome failures in addition to those we have described, our position is to be very skeptical of the debris avalanches proposed by these authors. Likewise, we are skeptical of the recurrence intervals proposed for large debris avalanches (e.g. 30–340 years between 120 and 970 AD) and believe them to be generally too short.

Acknowledgements We are grateful to the tephrochronology experts of the region, M. Pevzner and V. Ponomareva, for useful consultations. We thank L. Sulerzhitsky for radiocarbon dating of soil samples. The SEM analyses of pyroclasts, and preparation of the manuscript, were made during a postdoctoral fellowship of A.B. and M.B. at Pennsylvania State University. The paper was improved by critical reviews provided by D. A. Swanson and L. Siebert. This research was supported partly by NSF grant 96-14622 and by grant RG1-172 of the U.S. Civilian Research and Development Foundation and the Russian Government.

References

- Beget J, Kienle J (1992) Cyclic formation of debris avalanches at Mount St. Augustine Volcano. *Nature* 356:701–704
- Belousov AB (1995) The Shiveluch volcanic eruption of 12 November 1964: explosive eruption provoked by failure of the edifice. *J Volcanol Geotherm Res* 66:357–365
- Belousov AB (1996) Pyroclastic deposits of March 30, 1956 directed blast at Bezymianny volcano. *Bull Volcanol* 57:649–662
- Belousov AB, Bogoyavlenskaya GE (1988) Debris avalanche of the 1956 Bezymianny eruption. *Proc Kagoshima Int Conf on Volcanoes*, pp 460–462
- Belousov AB, Belousova MG (1996) Large scale landslides on active volcanoes in the twentieth century: examples from the Kurile-Kamchatka region (Russia). In: Senneset K. (ed) *Landslides*. Balkema, Rotterdam, pp. 953–957
- Belousov AB, Belousova MG (1998) Bezymyanni eruption on March 30, 1956 (Kamchatka): sequence of events and debris-avalanche deposits. *Volcanol Seismol* 20:29–49
- Belousova MG (1994) Deposits of large-scale edifice failures at volcanoes of Kamchatka and Kuril islands. PhD dissertation, Moscow State University (in Russian)
- Belousova MG (1996) Large-scale edifice failures and associated eruptions in the history of Shiveluch volcano (Kamchatka). *Proc Moscow Univ Geol Issue 2*:23–26 (in Russian)
- Belousova MG, Belousov AB (1994a) The history of Shiveluch volcano (Kamchatka): an example of extreme edifice instability. Abstracts of conference on volcano instability, London, p 2
- Belousova MG, Belousov AB (1994b) Repetitive, magma driven, large-scale edifice failures of Shiveluch volcano (Kamchatka). Abstracts of the IAVCEI General Assembly, Ankara, Turkey
- Braitseva OA, Kirianov VY, Sulerzhitsky LD (1989) Marker intercalations of Holocene tephra in the Eastern volcanic zone of Kamchatka. *Volcanol Seismol* 7:785–814
- Braitseva OA, Melekestsev IV, Ponomareva VV, Sulerzhitsky LD (1992) Tephra of the largest prehistoric Holocene volcanic eruptions in Kamchatka. *Quaternary Int* 13/14:177–180
- Braitseva OA, Melekestsev IV, Ponomareva VV, Sulerzhitsky LD (1995) Ages of calderas, large explosive craters and active volcanoes in the Kuril-Kamchatka region, Russia. *Bull Volcanol* 57:383–402
- Castellana B, Davidson JP, Belousov A, Belousova M (1995) Milestones of geology of the Avachinskiy volcano, Kamchatka, Russia. *EOS Trans* 76:537
- Dril SI (1988) The origin and evolution of andesites of island arcs (Zavaritsky, Ebeko volcanoes at Kurile islands and Shiveluch volcano at Kamchatka). PhD dissertation, Moscow State University (in Russian)
- Dvigalo VN (1995) Lava dome development in the Shiveluch crater (Kamchatka) during 1980–1995 through the data on photogrammetric observations. *Proc Int Workshop on Mt Showa-Shinzan*, p 30
- Firstov PP, Gavrilov YuA, Zhdanova EYu, Kirianov VYu (1995) New extrusive eruption of Shiveluch in April 1993. *Volcanol Seismol* 16:371–387
- Francis PW, Wells GL (1988) Landsat Thematic Mapper observations of debris-avalanche deposits in the Central Andes. *Bull Volcanol* 50:258–278
- Glicken H (1986) Rockslide-debris avalanche of the May 18, Mount St. Helens, Washington. PhD dissertation, Univ Calif Santa Barbara, 303 pp
- Glicken H (1991) Sedimentary architecture of large-volcanic debris avalanches. *Soc Econ Paleontol Mineral Spec Publ* 45:99–106
- Glicken H (1998) Rockslide-debris avalanche of May 18, 1980, Mount St. Helens volcano, Washington. *Bull Geol Soc Japan* 49:55–106
- Gorshkov GS (1959) Gigantic eruption of the volcano Bezymianny. *Bull Volcanol* 20:77–109
- Gorshkov GS, Dubik YM (1970) Gigantic directed blast at Shiveluch volcano (Kamchatka). *Bull Volcanol* 34:262–288
- Hoblitt RV, Miller CD, Vallance JW (1981) Origin and stratigraphy of the deposit produced by the May 18 directed blast. In: Lipman PW, Mullineaux DR (eds) *The 1980 eruptions of Mount St. Helens, Washington*. US Geol Surv Prof Pap 1250:401–419
- Inman DL (1952) Measures for describing the size distribution of sediments. *J Sed Petrol* 22:125–145
- Inokuchi T (1988) Gigantic landslides and debris avalanches on volcanoes in Japan: case studies on Bandai, Chokai and Iwate Volcanoes. *Rep Nat Res Center Disaster Prevention* 41:163–275 (in Japanese with English abstract)

- Komorowski JC, Glicken H, Sheridan MF (1991) Secondary electron imagery of microcracks and hackly fractures in sand-size clasts from the 1980 Mount St. Helens debris-avalanche deposits, implications for particle-particle interactions. *Geology* 19:261–264
- Komorowski JC, Navarro C, Cortes A, Siebe C, Rodriguez S (1993) Recurrent collapse of Volcan Colima (Mexico) since 10000 years BP: implications for eruptive processes, magma output, edifice stability and volcanic risks. Abstracts of IAVCEI General Assembly, Canberra, p 60
- Krahmalev I (1880) Kamchatkan volcano Kluchevskaya fire-breathed hill. *Irkutsk Eparhial lists* 9 (in Russian)
- Krashenninnikov S (1755) Descriptions of the land of Kamchatka. *Imperator Acad Sci, Saint-Petersburg* (in Russian)
- Melekestsev IV, Braitseva OA, Erlih ON, Kozhemiaka NN (1974) Volcanic mountains and plains. In: Luchitsky IV (ed) *Kamchatka, Kuril and Commander islands*. Nauka, Moscow, pp 162–234 (in Russian)
- Melekestsev IV, Volynets ON, Yermakov VA, Kirsanova TP, Masurenkov YP (1991) Sheveluch volcano. In: Fedotov SA, Masurenkov YP (eds) *Active volcanoes of Kamchatka*. Nauka, Moscow, pp 84–105
- Menyailov AA (1955) Shiveluch volcano, its geological structure, composition and eruptions. *Trans Volcan Lab USSR Acad Sci* 9 (in Russian)
- Moore JG, Sisson TW (1981) Deposits and effects of the May 18 pyroclastic surge. *US Geol Surv Prof Pap* 1250:421–438
- Moore JG, Clague DA, Holcomb RT, Lipman PW, Normark WR, Torresan ME (1989) Prodigious submarine landslides on the Hawaiian Ridge. *J Geophys Res* 94:465–484
- Mori J, McKee C, Talai B, Itikarai I (1989) A summary of precursors to volcanic eruptions in Papua New Guinea. In: Latter JH (ed) *Volcanic hazards*. Springer, Berlin Heidelberg New York, pp 260–291
- Ponomareva VV, Pevzner MM, Melekestsev IV (1998) Large debris avalanches and associated eruptions in the Holocene eruptive history of Shiveluch volcano, Kamchatka, Russia. *Bull Volcanol* 59:490–505
- Sekiya S, Kikuchi Y (1889) The eruption of Bandai-san. *Tokyo Imp Univ Coll Sci J* 3:91–172
- Shaller PJ (1991a) Analysis and implication of large martian and terrestrial landslides. PhD dissertation, California Institute of Technology
- Shaller PJ (1991b) Analysis of a large moist landslide, Lost River range, Idaho, USA. *Can Geotech J* 28:584–600
- Siebe C, Komorowski J-C, Sheridan MF (1992) Morphology and emplacement of an unusual debris-avalanche deposit at Jocotitlan volcano, Central Mexico. *Bull Volcanol* 54:573–589
- Siebert L (1984) Large volcanic debris avalanches: characteristics of source areas, deposits, and associated eruptions. *J Volcanol Geotherm Res* 22:163–197
- Siebert L (1996) Hazards of large volcanic debris avalanches and associated eruptive phenomena. In: Scarpa R, Tilling RI (eds) *Monitoring and mitigation of volcano hazard*, Springer, Berlin Heidelberg New York, pp 541–572
- Siebert L, Glicken H, Ui T (1987) Volcanic hazards from Bezymianny- and Bandai-type eruptions. *Bull Volcanol* 49:435–459
- Siebert L, Beget J, Glicken H (1995) The 1883 and late-prehistoric eruptions of Augustine volcano, Alaska. *J Volcanol Geotherm Res* 66:367–395
- Ui T (1983) Volcanic dry avalanche deposits: identifications and comparison with nonvolcanic debris stream deposits. *J Volcanol Geotherm Res* 18:135–150
- Voight B, Elsworth D (1997) Failure of volcano slopes. *Geotechnique* 47:1–31
- Voight B, Sousa J (1994) Lessons from Ontake-san: a comparative analysis of debris avalanche dynamics. *Eng Geol* 38:261–297
- Voight B, Glicken H, Janda RJ, Douglass PM (1981) Catastrophic rockslide avalanche of May 18. In: Lipman PW, Mullineaux DR (eds) *The 1980 eruptions of Mount St. Helens*, Washington. *US Geol Surv Prof Pap* 1250:347–377
- Voight B, Janda RJ, Glicken H, Douglass PM (1983) Nature and mechanics of the Mount St. Helens rockslide-avalanche of the 18 May 1980. *Geotechnique* 33:243–273
- Wadge G, Francis P, Ramirez (1995) The Socompa collapse and avalanche event. *J Volcanol Geotherm Res* 66:309–336
- Waitt RB (1981) Devastating pyroclastic density flow and attendant air fall of May 18: stratigraphy and sedimentology of deposits. *US Geol Surv Prof Pap* 1250:439–458
- Walker GPL (1971) Grain-size characteristics of pyroclastic deposits. *J Geol* 79:696–714